MultiInv: Inverting Multidimensional Scaling Projections and Computing Decision Maps by Multilateration – Appendix

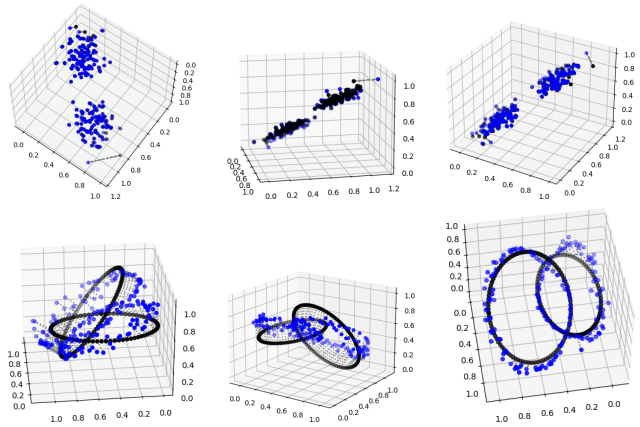

Figure 1: 3D plot of original data (black) and inverse projection (blue) for the *Plane* (top row) and *Rings* (bottom row) dataset from different angles. Original data samples and respective inverse projected counterparts are connected by a dashed line. For the inverse projection, our proposed multilateriation-based technique *MultiInv* is used with MDS as direct projection.

Full-page figures are located on the following pages.

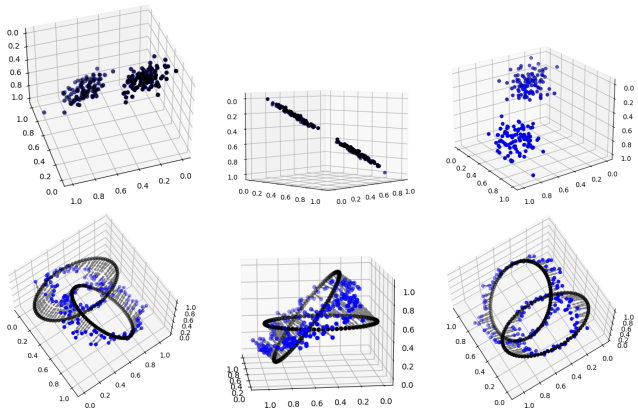

Figure 2: 3D plot of original data (black) and inverse projection (blue) for the *Plane* (top row) and *Rings* (bottom row) dataset from different angles. Original data samples and respective inverse projected counterparts are connected by a dashed line. For the inverse projection, our proposed multilateriation-based technique *MultiInv* is used with PCA as direct projection.

Dataset	*Ours - random*				*Ours - filtered*				iLAMP				iNN				RBF			
	min	max	mean	median	min	max	mean	median	min	max	mean	median	min	max	mean	median	min	max	mean	median
Plane	0.87	28.08	3.11	2.39	0.95	20.03	2.61	2.1	0.35	182.7	12.93	3.36	0.46	2.16	1.30	1.34	0.76	2.59	1.34	1.36
Rings	0.65	421.03	10.65	8.27	0.55	695.51	11.2	8.50	0.13	102.09	10.97	5.63	0.77	5.96	1.57	1.43	0.8	16.07	1.68	1.54
Blobs	7.49	174.60	47.69	43.70	7.61	118.78	37.93	34.91	0.84	94.52	11.17	8.09	0.52	16.37	3.08	2.52	1.27	37.55	4.02	3.05
Iris	0.95	115.81	9.65	7.89	1.01	363.17	7.24	6.06	0.51	189.53	14.21	5.09	0.81	3.95	1.43	1.39	0.83	7.65	1.66	1.44
Seismic	161.14	4835.13	1372.55	1316.92	114.58	3996.04	1092.53	1031.27	0.60	98.32	11.16	7.68	0.09	11.44	2.5	2.05	1.03	26.27	3.21	2.64
Bank	263.53	2292.62	1032.25	1041.07	221.26	1936.83	869.37	874.21	0.31	85.91	18.29	17.12	0.62	23.51	4.0	3.46	1.10	63.80	13.49	13.00

Table 1: Gradient values for *MultiInv* applied to six datasets projected by MDS. Values are rounded to the second decimal place.

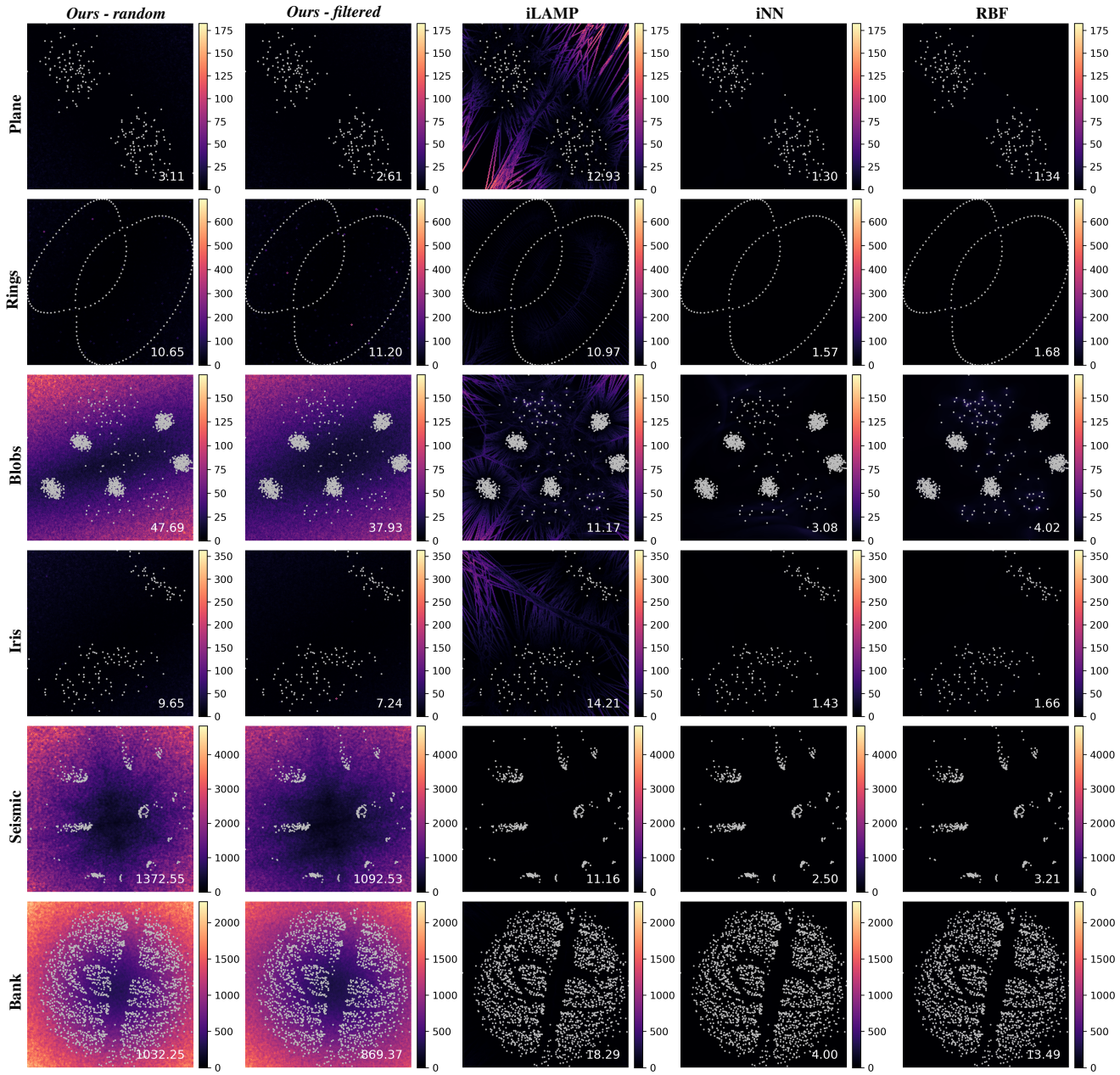

Figure 3: Gradient maps of inverse projections for each of the six datasets projected using MDS. The color scale is unified for each dataset, with the minimum being set to 0 and the maximum to the maximum gradient of the approaches. Darker colors indicate a low rate of change, and lighter areas show a high rate of change. The number at the bottom right shows the average gradient.

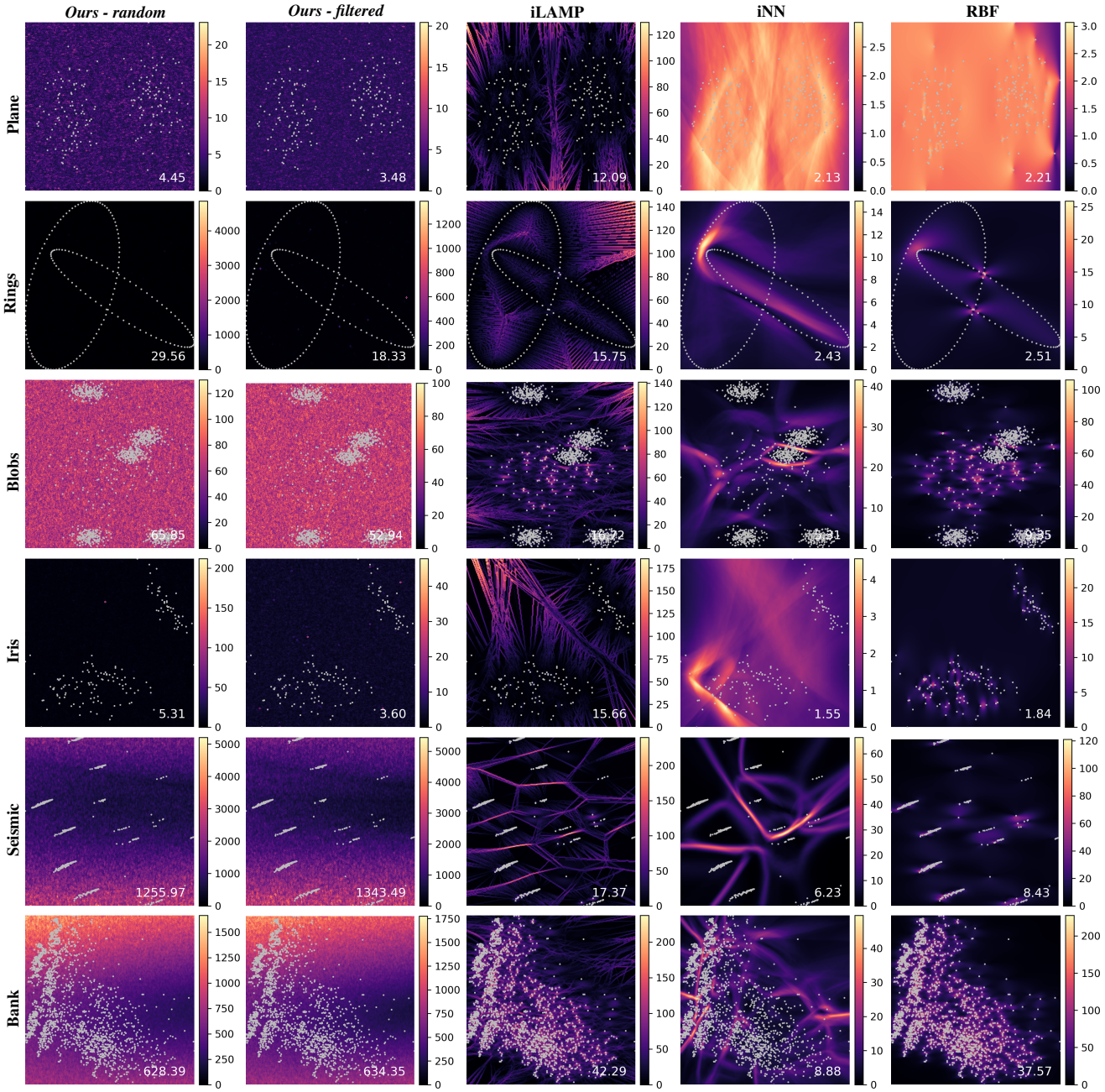

Figure 4: Gradient maps of inverse projections for six datasets projected using CCA. Darker colors indicate a low rate of change, and lighter areas show a high rate of change. The number at the bottom right shows the average gradient.

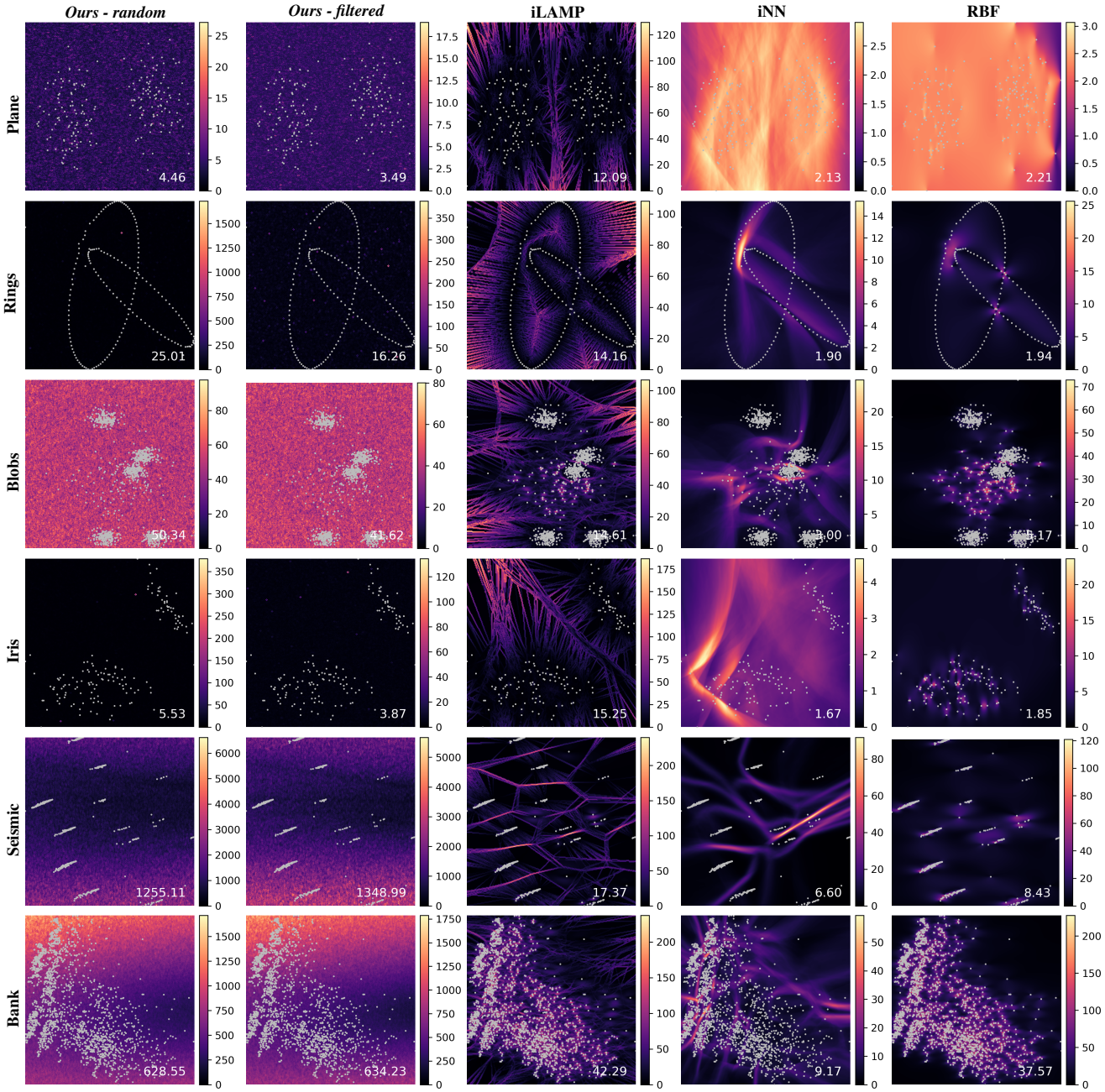

Figure 5: Gradient maps of inverse projections for six datasets projected using Sammon's mapping. Darker colors indicate a low rate of change, and lighter areas show a high rate of change. The number at the bottom right shows the average gradient.

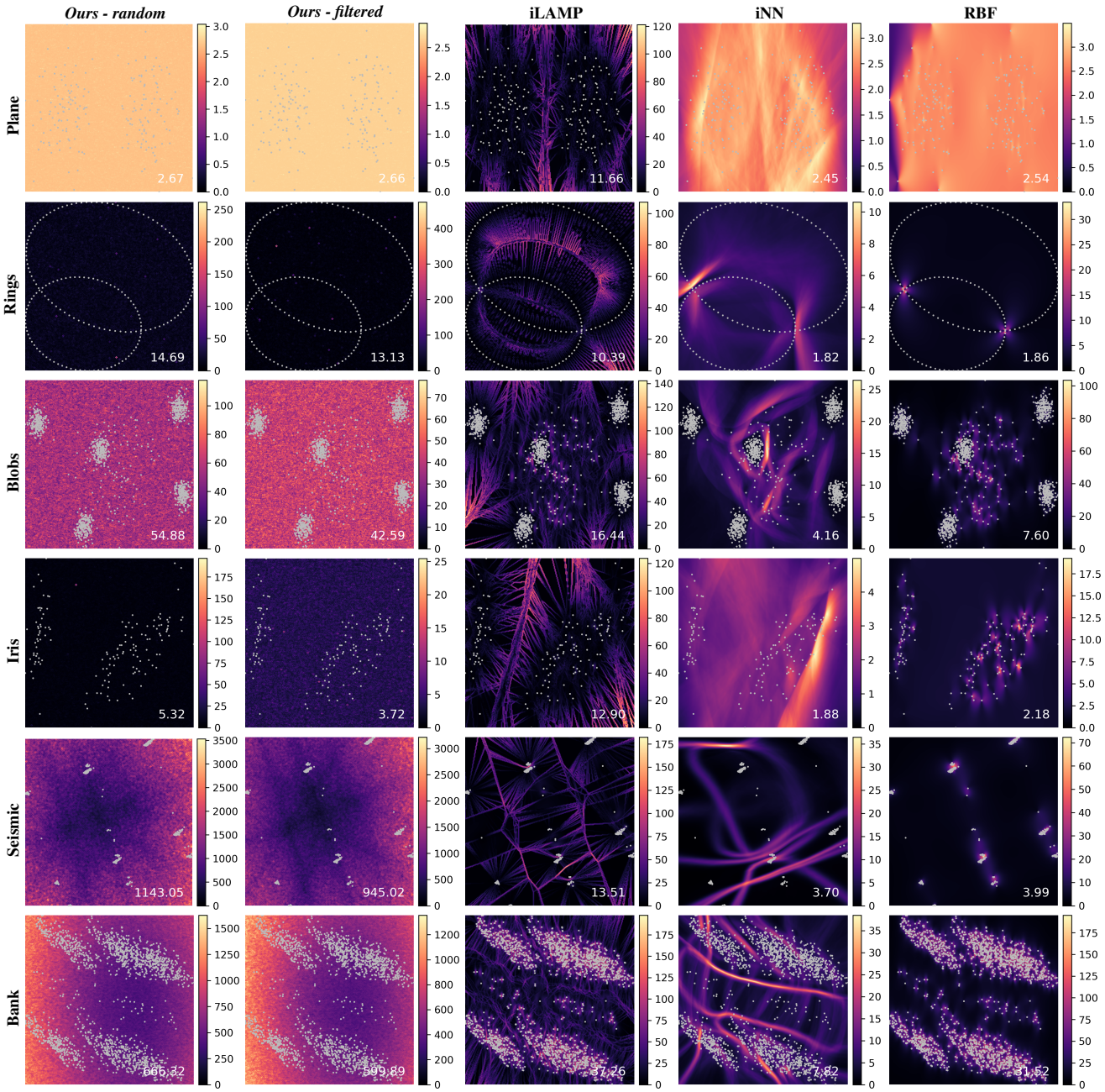

Figure 6: Gradient maps of inverse projections for six datasets projected using PCA. Darker colors indicate a low rate of change, and lighter areas show a high rate of change. The number at the bottom right shows the average gradient.

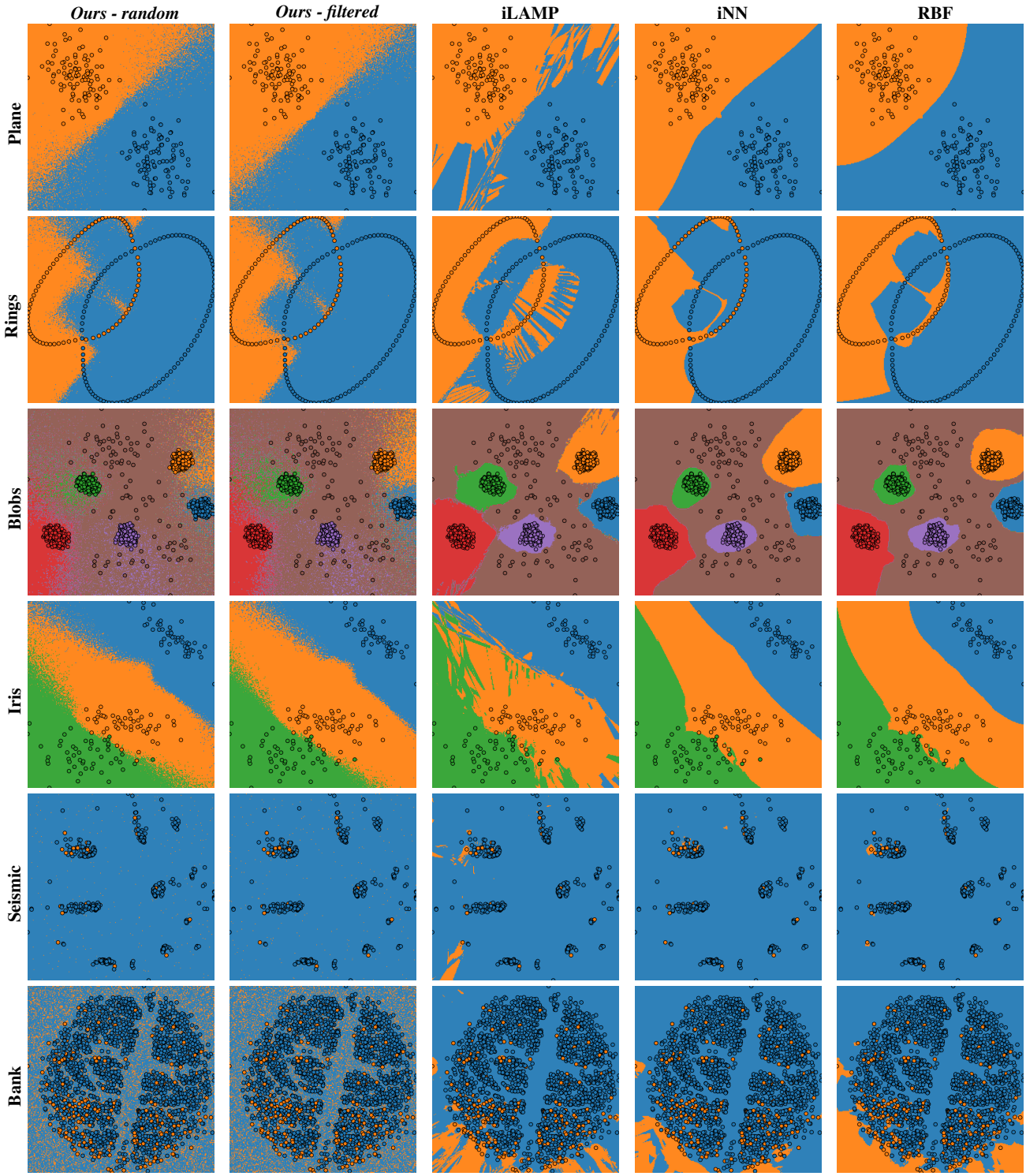

Figure 7: Decision maps of inverse projections for six datasets projected using MDS and classified by a random forest classifier.

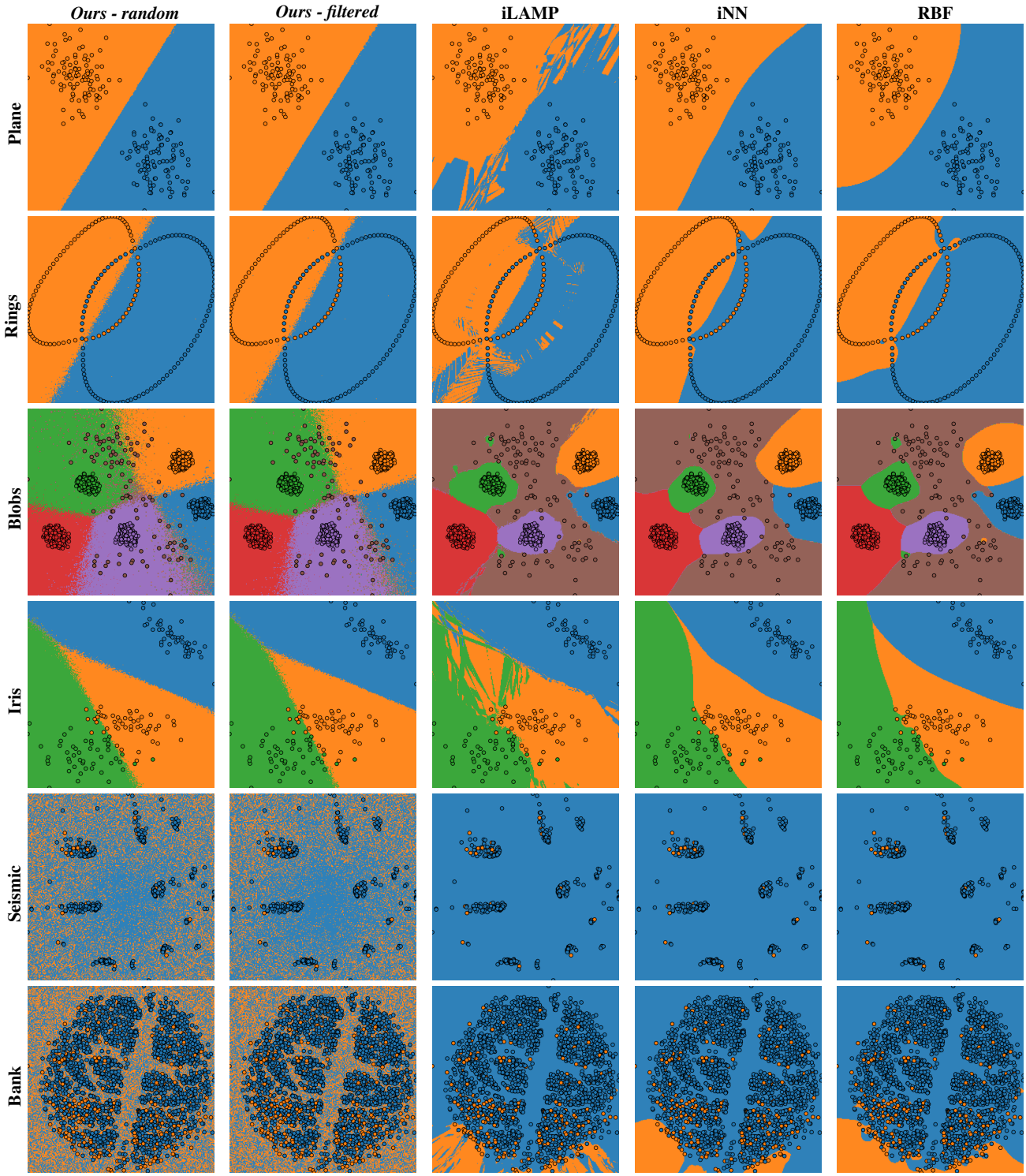

Figure 8: Decision maps of inverse projections for six datasets projected using MDS and classified by a logistic regression classifier.

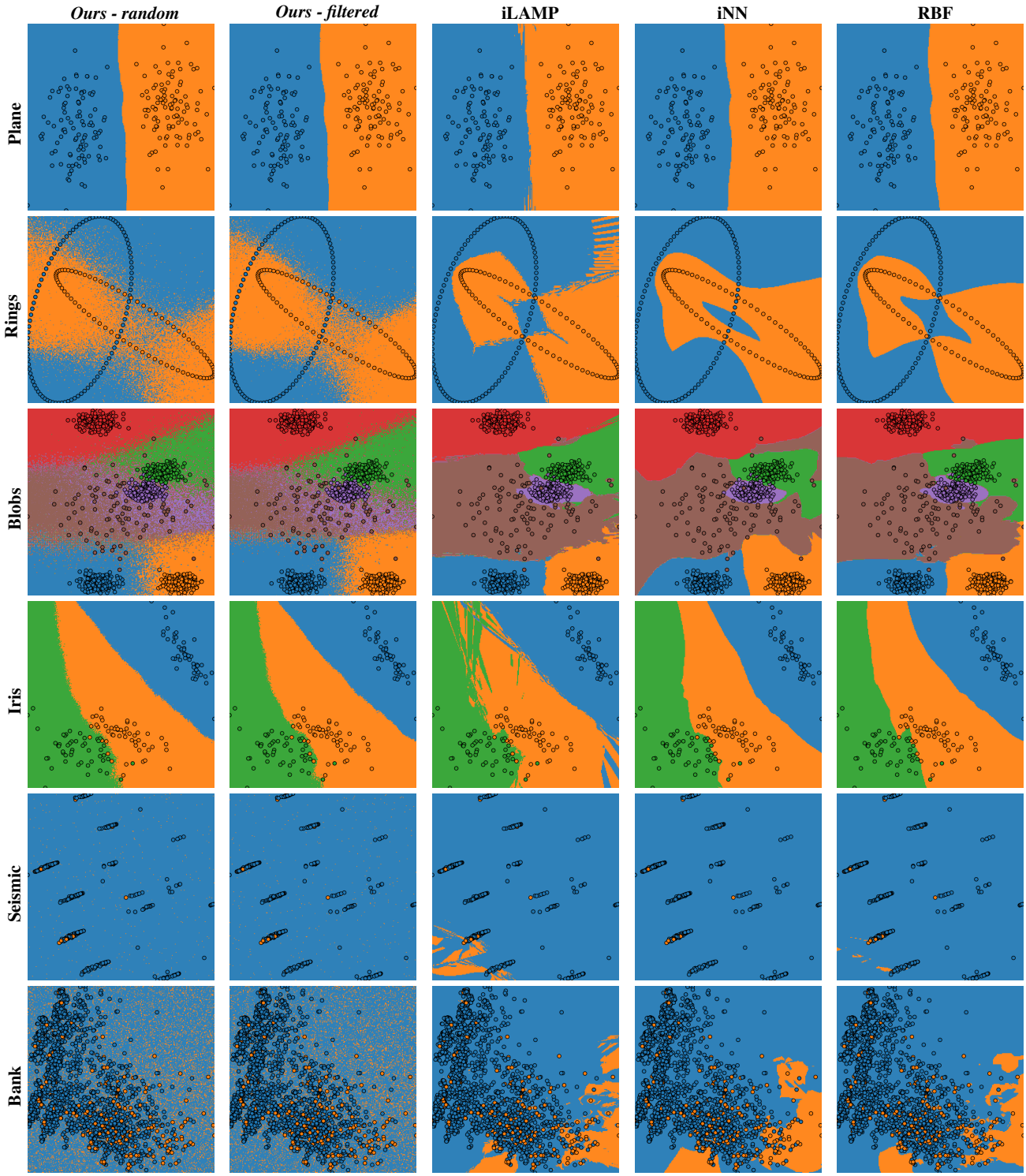

Figure 9: Decision maps of inverse projections for six datasets projected using CCA and classified by a k-nearest neighbor classifier with k=5.

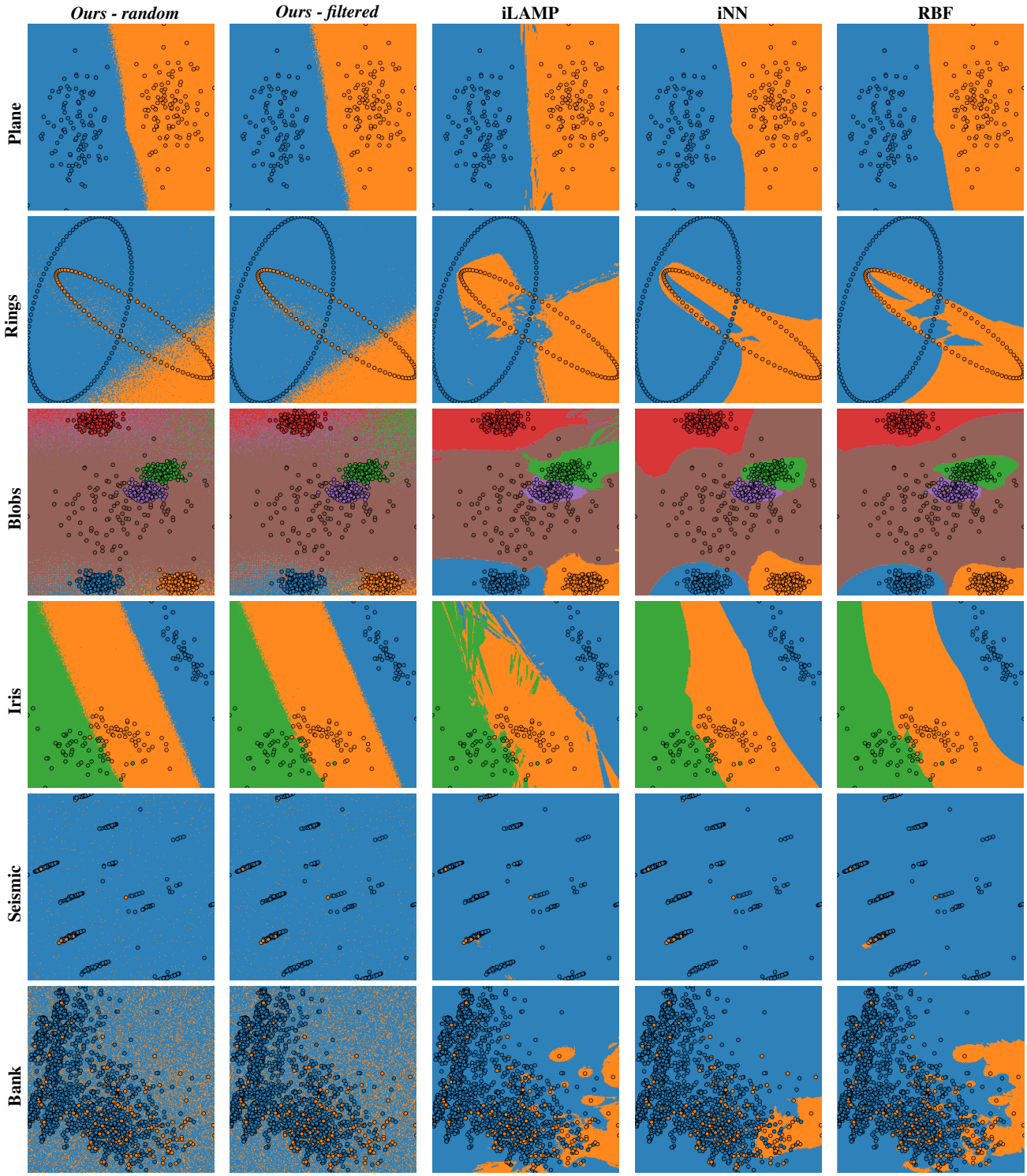

Figure 10: Decision maps of inverse projections for six datasets projected using CCA and classified by a random forest classifier.

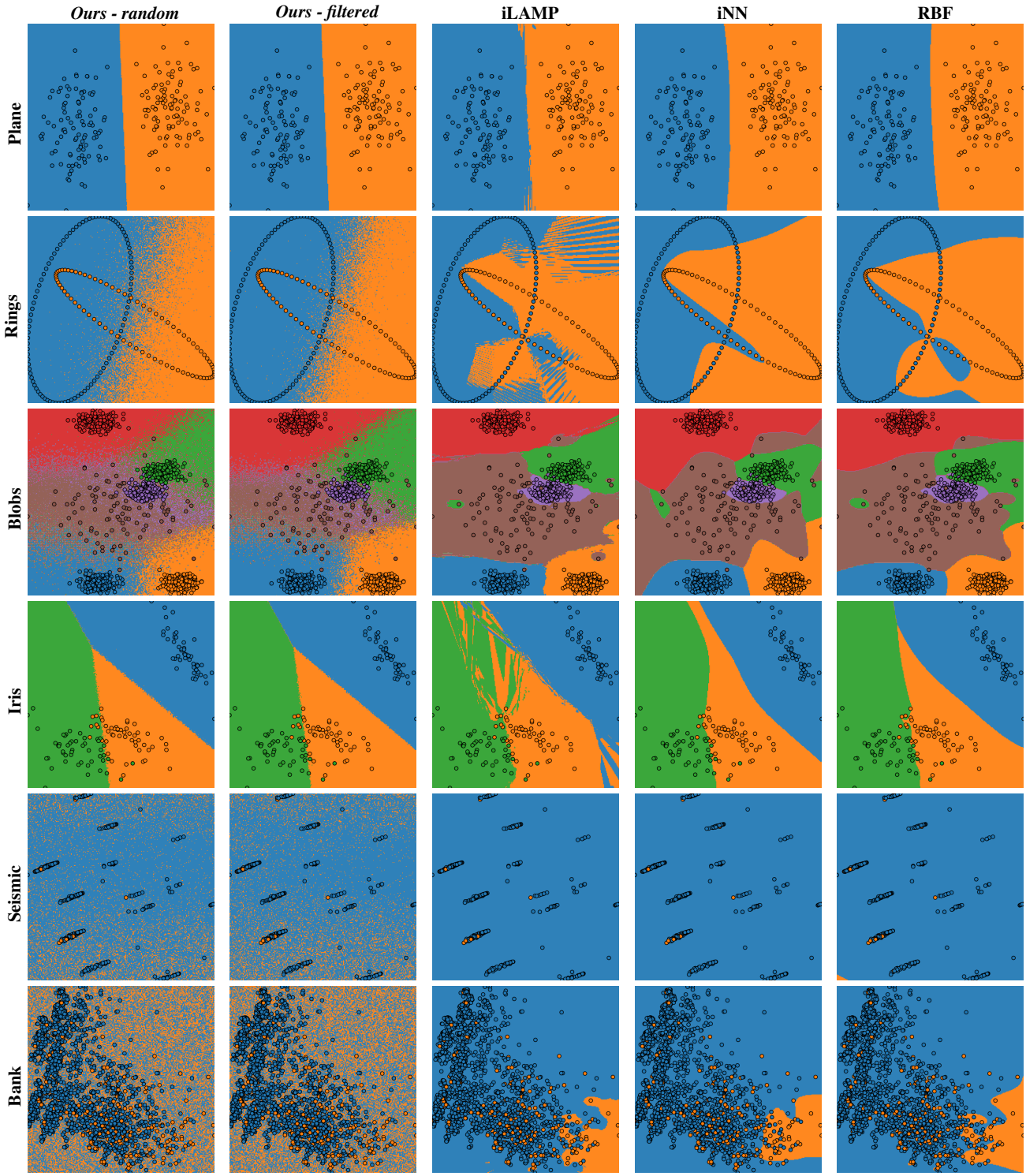

Figure 11: Decision maps of inverse projections for six datasets projected using CCA and classified by a logistic regression classifier.

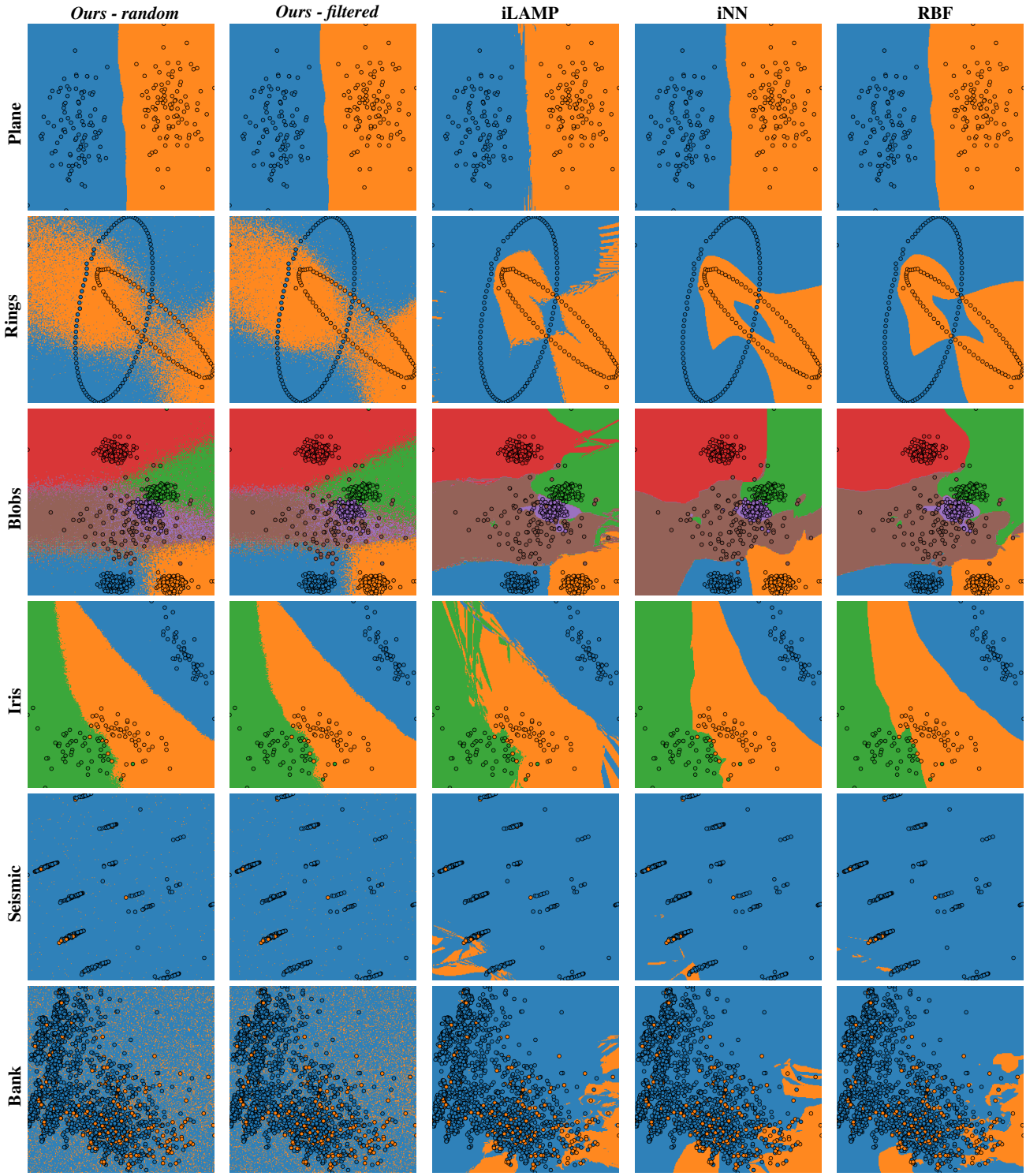

Figure 12: Decision maps of inverse projections for six datasets projected using Sammon's mapping and classified by a k-nearest neighbor classifier with k=5.

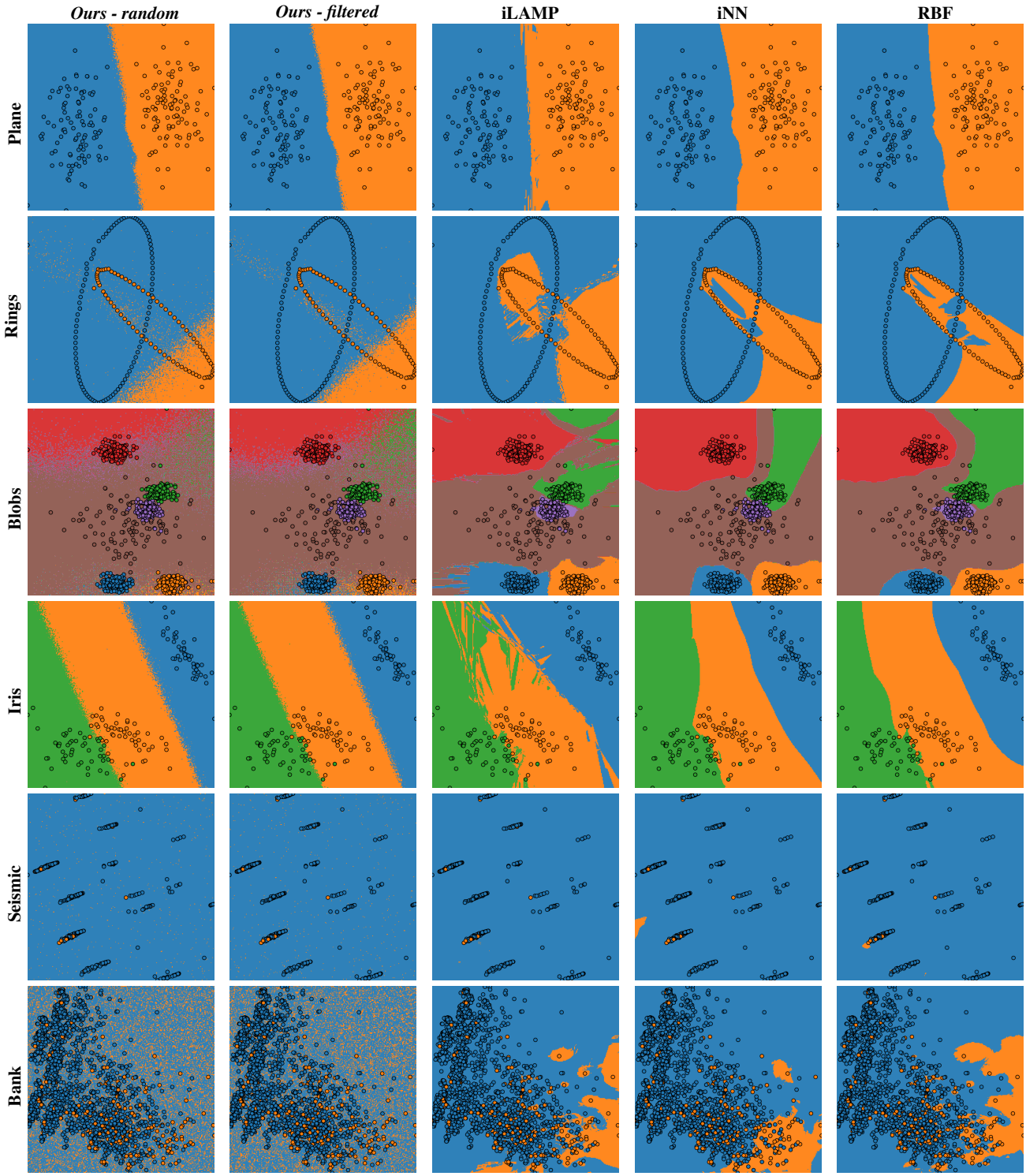

Figure 13: Decision maps of inverse projections for six datasets projected using Sammon's mapping and classified by a random forest classifier.

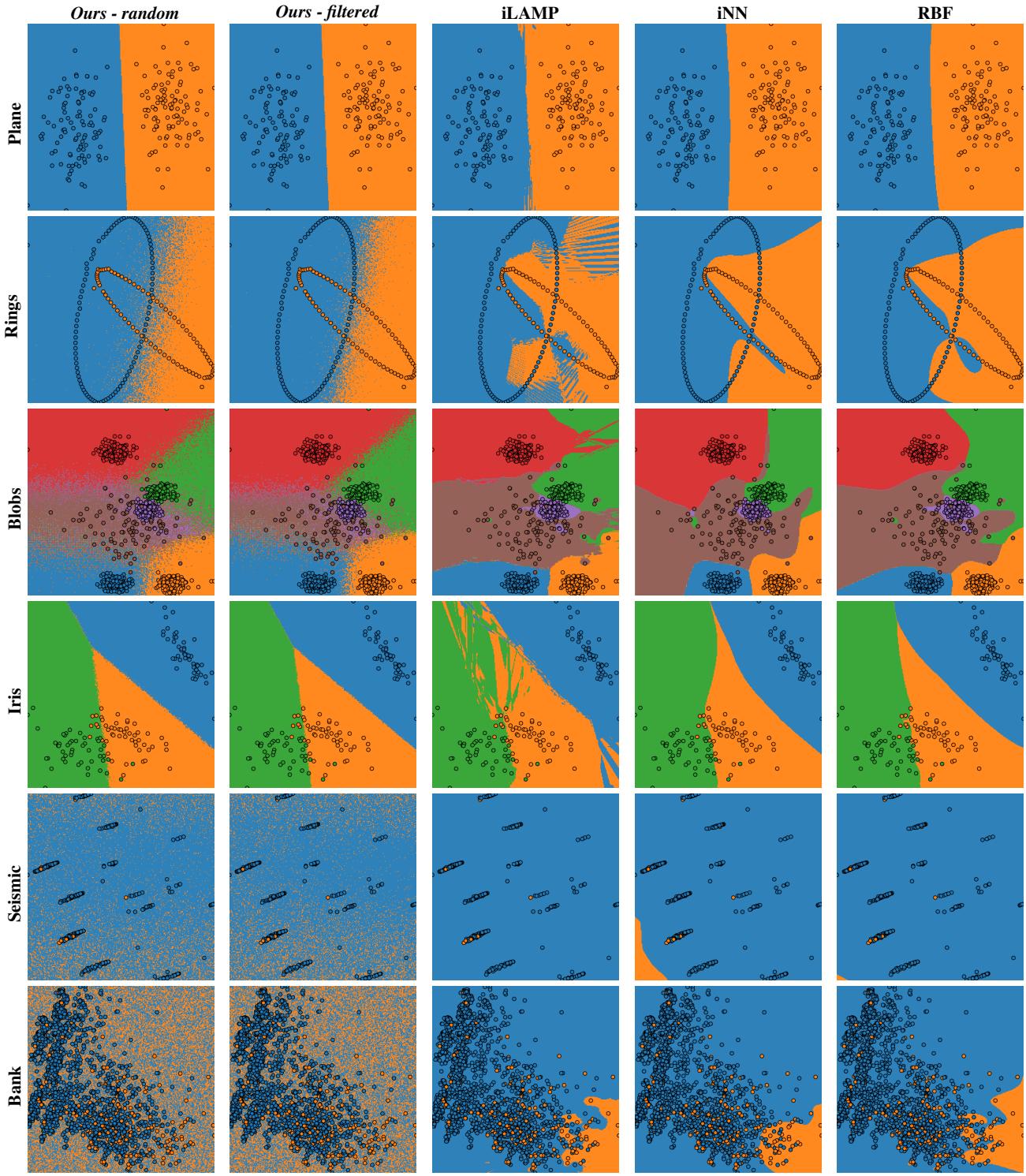

Figure 14: Decision maps of inverse projections for six datasets projected using Sammon's mapping and classified by a logistic regression classifier.

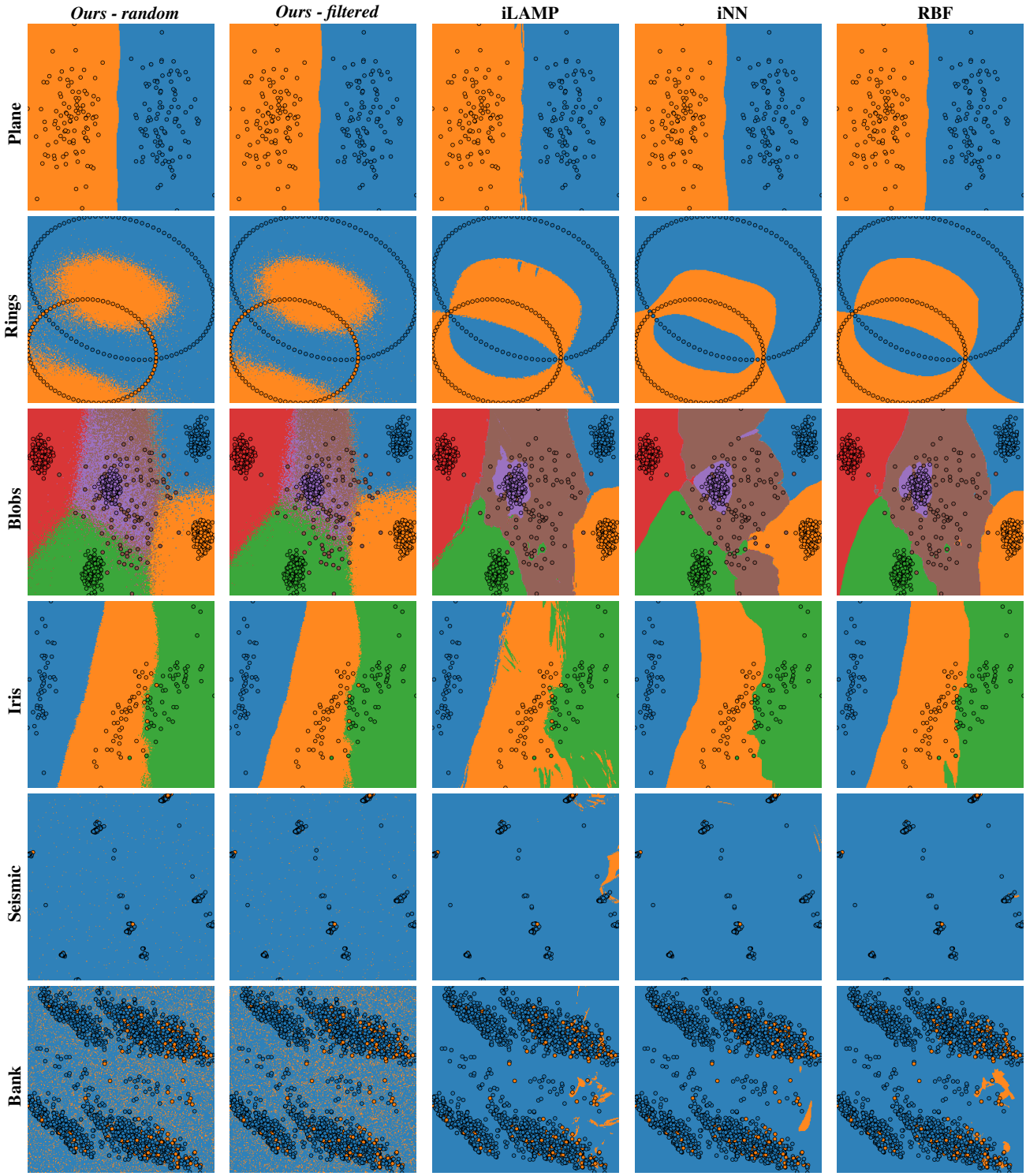

Figure 15: Decision maps of inverse projections for six datasets projected using PCA and classified by a k-nearest neighbor classifier with k=5.

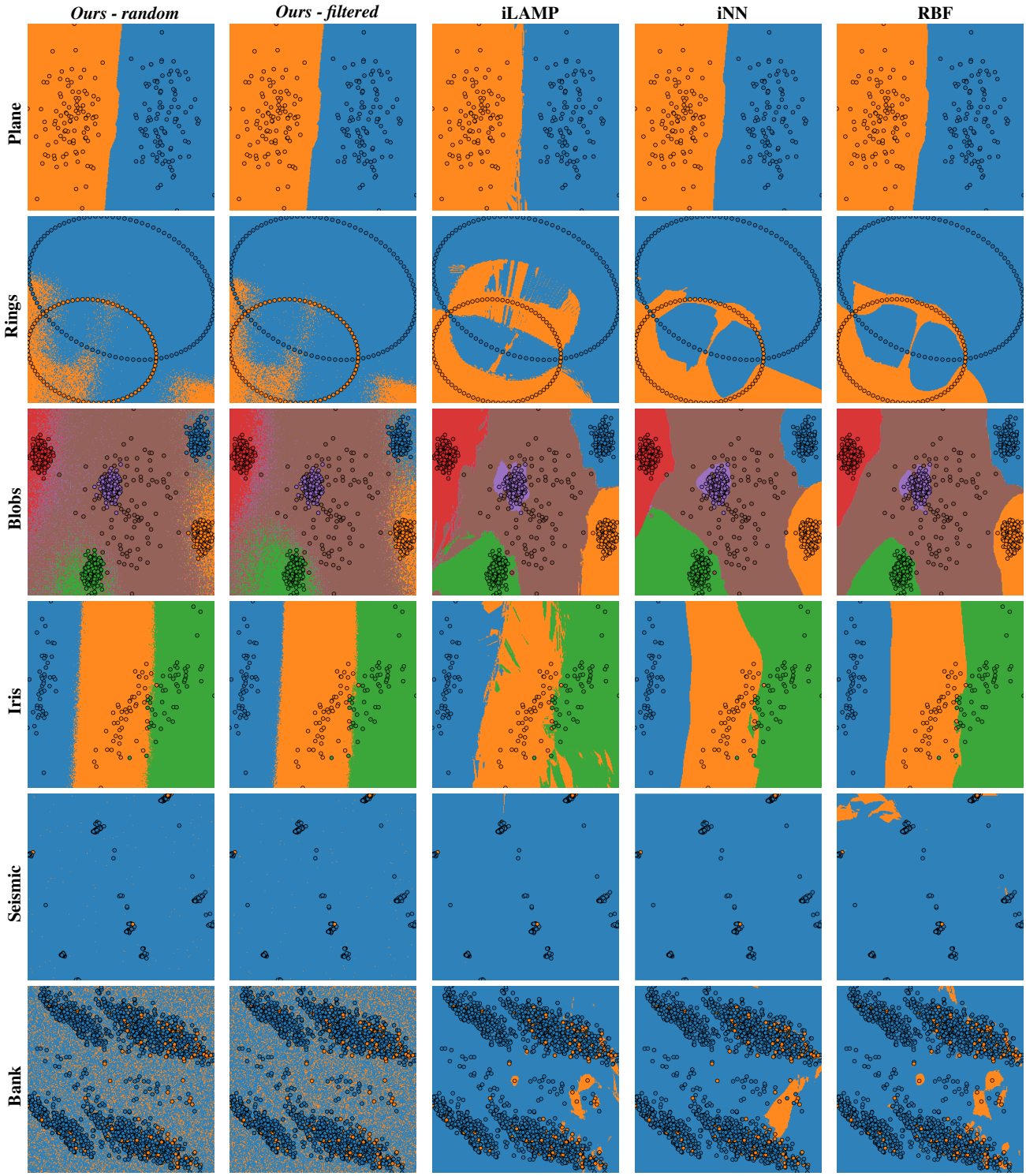

Figure 16: Decision maps of inverse projections for six datasets projected using PCA and classified by a random forest classifier.

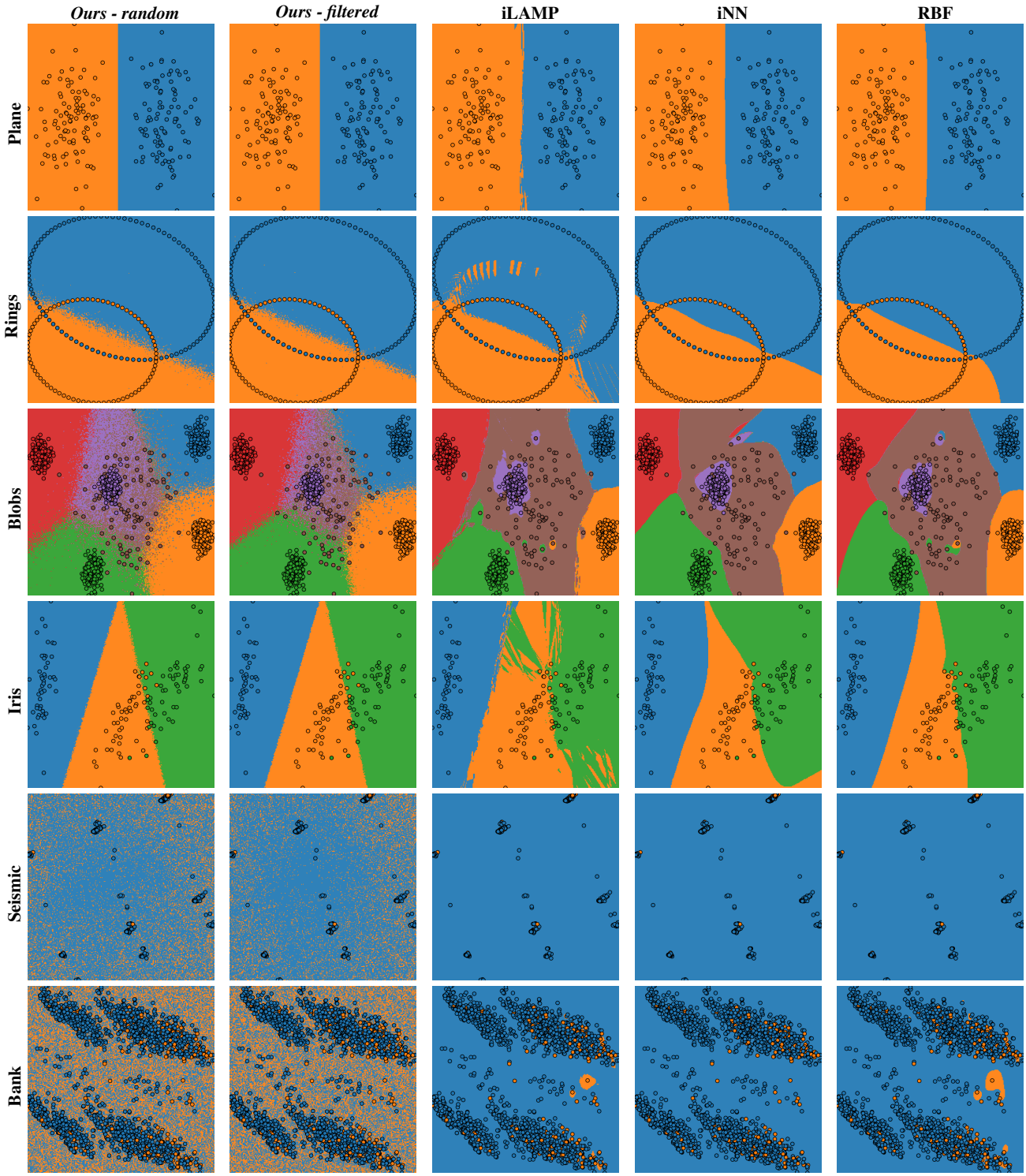

Figure 17: Decision maps of inverse projections for six datasets projected using PCA and classified by a logistic regression classifier.

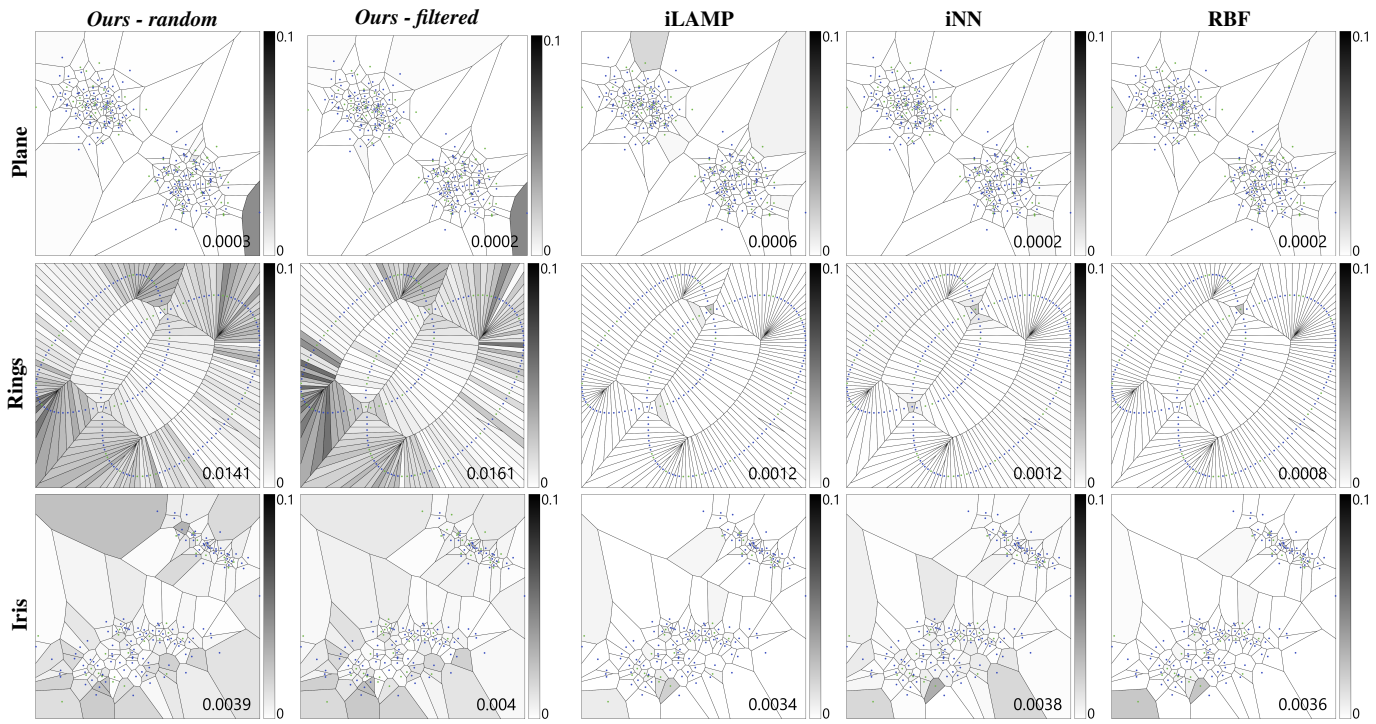

Figure 18: Comparison of inverse projections showing the MSE for known points encoded in Voronoi cells associated with each projected sample of three datasets when applying MDS. The number at the bottom right corner indicates the average MSE for the test samples (20% of the dataset; colored in green).